Original Article

Journal of Drought and Climate change Research (JDCR)

Winter 2025, Vol. 2, No. 8, pp 121-140

10.22077/jdcr.2025.8636.1098

Development of Intensity-Duration-Frequency Curves at Basin Scale using the ERA5 Reanalysis Product

Ameneh Mianabadi[1], Javad Omidvar[2], Mohsen Pourreza-Bilondi[3*]

1- Department of Ecology, Institute of Science and High Technology and Environmental Sciences, Graduate University of Advanced Technology, Kerman, Iran.
2- Department of Water Sciences and Engineering, Faculty of Agricultural, Ferdowsi University of Mashhad, Mashhad, Iran.
3- Department of Water Engineering, University of Birjand, Birjand, Iran.
*** corresponding author: Mohsen.pourreza@birjand.ac.ir**

Keywords:
Annual Maximum Precipitation, Bias Correction, Climate Change, Flood Management, Karkheh River Basin.

Received:
25 Dec 2024

Revised:
5 Feb 2025

Accepted:
7 Feb 2025

Abstract

Intensity-Duration-Frequency (IDF) curves are essential for hydrological modeling, infrastructure design, and flood risk management. However, traditional methods of IDF curve development relying on ground-based observations face significant limitations, including sparse spatial coverage, short temporal records, and the stationary assumption, particularly in the context of climate change. Accordingly, this study addresses these challenges by utilizing ERA5 reanalysis data to develop basin-scale IDF curves for the Karkheh River Basin (KRB) in Iran. The Annual Maximum Precipitation (AMP) series for durations of 6-, 12-, 18-, and 24-hours were extracted from ERA5 data and corrected for bias using observed precipitation from seven synoptic stations. The bias correction significantly improved ERA5 estimates, especially in high-altitude regions. A relationship between elevation and bias factors was established to extend the correction across the basin. The corrected AMP data were then modeled using the Generalized Extreme Value (GEV) distribution, considering both stationary and non-stationary conditions, to construct spatially distributed IDF curves based on 82 grid points across the basin. The spatial maps of IDF indicate that rainfall intensity varies

How to cite this article:
Mianabadi, A., Omidvar. J., & Pourreza-Bilondi. M. (2024). Development of Intensity-Duration-Frequency Curves at Basin Scale using the ERA5 Reanalysis Product. *Journal of Drought and Climate change Research* (JDCR), 2(8), 121-140. 10.22077/jdcr.2025.8636.1098

significantly across the basin, with higher intensities observed in elevated regions. These maps provide detailed and reliable rainfall intensity estimates compared to traditional station-based methods. This work highlights the potential of ERA5 data, combined with robust bias correction, to enhance hydrological analysis in data-scarce regions.

Introduction

Accurate estimation of extreme rainfall events is crucial for the design and planning of various critical infrastructures, including urban drainage systems, dams, and bridges (Venkatesh et al., 2022). These structures must be designed to withstand the impacts of intense rainfall events, which can lead to flooding and other significant consequences. Intensity-Duration-Frequency (IDF) curves provide a valuable tool for characterizing these extreme events by relating rainfall intensity to its duration and return period (Koutsoyiannis et al., 1998). Traditional methods for developing IDF curves primarily rely on historical rainfall data collected from ground-based rain gauges (Marra et al., 2017; Noor et al., 2021; Venkatesh et al., 2022). However, these methods often face significant limitations. Firstly, the spatial coverage of ground-based rain gauges is typically sparse, leading to inadequate representation of rainfall variability across a basin. This spatial sparsity can result in significant uncertainties in the derived IDF curves, particularly in regions with limited gauge networks (Noor et al., 2021). Secondly, the temporal record of ground-based observations is often relatively short, limiting the ability to capture the full range of extreme rainfall events, especially for the longer return periods (Marra et al., 2017). Thirdly, the assumption of stationary, which assumes that the statistical properties of rainfall remain constant over time, may be rendered invalid due to the impacts of climate change (IPCC, 2021). Finally, the distance of the designed infrastructures from the gauges' location decreases the effectiveness of the gauge-acquired IDF curves (Marra et al., 2017). These limitations lead the researcher to apply alternative data sources such as global gridded precipitation products for IDF development (Wambura, 2024).

In addition to the mentioned challenges, the point-based IDF curves may not adequately capture spatial variations in rainfall intensity, especially in large or topographically diverse regions (Marra et al., 2017). To overcome this issue, the development of spatially-distributed IDF curves has gained attention. Spatial IDF curves utilize gridded datasets to provide continuous coverage over a region, offering more detailed and reliable information for infrastructure design and flood management. The emergence of high-resolution reanalysis datasets, such as

ERA5 (Hersbach et al., 2020), has provided a promising alternative for developing IDF curves (Hersbach et al., 2023). The ERA5 dataset, produced by the European Centre for Medium-Range Weather Forecasts (ECMWF), provides a globally consistent and spatially comprehensive record of atmospheric variables, including precipitation. The high temporal resolution of this product (hourly to daily available data) , make it suitable for developing IDF curves in data-scarce basins (Tarek et al., 2020).

Few studies used the ERA5 data to develop the IDF curves at global (Courty et al., 2019) and regional scales (Jalbert et al., 2022; Wambura, 2024; Zambrano-Bigiarini et al., 2024). Among them, Jalbert et al. (2022) provided a map of spatial rainfall intensity for 25-year return period for 30-min rainfall. This study aims to assess the feasibility and accuracy of utilizing ERA5 reanalysis data for IDF curve development at the basin scale by establishing an explicit relationship between elevation and bias factor as describe in Materials and Methods section. The study also investigates potential improvements in spatial coverage and characterization of extreme rainfall events in regions with complex topography. Such integration of elevation-based corrections with ERA5 data and providing the spatial distribution of rainfall intensity for different durations and return periods have not been widely explored. Hence, this study represents a significant advancement in this filed.

Materials and Methods

Study Area

The Karkheh River Basin (KRB) with an area of approximately 51,000 km^2 is located in the southwest of Iran (Figure 1). The mean annual precipitation over the basin varies between about 250 mm in the southern part and up to 700 mm in the northern part (Ashraf Vaghefi et al., 2014). The Karkheh River originates from the Zagros mountains and goes firstly, to Hoor-Al-Azim Swamp (a transboundary wetland shared between Iran and Iraq), and then to Persian Gulf by connecting to Arvand Rud. The KRB holds great significance in the realms of both agriculture activities and energy generation. Karkheh Dam as the largest reservoir of Iran (> 5 billion cubic meters (BCM), has been constructed to provide water for these purposes (Davtalab et al., 2017).

ERA5 Data

ERA5, as the Fifth Generation of the European Centre for Medium-Range Weather Forecasts (ECMWF) Reanalysis, provides various meteorological variables data at global scale. The data are available from 1940 to present with a 0.25°×0.25° resolution (Hersbach et al., 2023). The hourly ERA5 precipitation data were downloaded from https://cds.climate.copernicus.eu/ (last access: 20/09/2023)

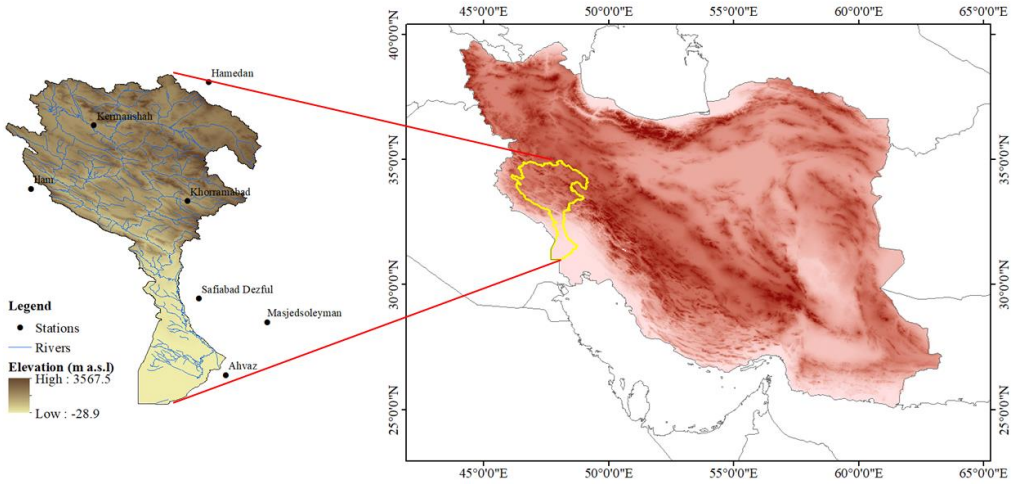

Fig 1. Geographical characteristics of the case study and the synoptic stations.

and then aggregated to the 6-, 12-, 18-, and 24-hourly precipitation data.

Observed Data

To validate the ERA5 data, we acquired the precipitation data from seven synoptic stations, within and around the watershed. The location of these stations has been shown in Figure 1. Due to limited access to the data, the quality-controlled 6-hourly precipitation data from 1996 to 2020 (25 years) were used for the analysis. The 12-, 18-, and 24-hourly precipitation data were acquired from the 6-hourly precipitation data.

Bias Correction

Previous investigations have demonstrated that the reanalysis products exhibit both random and systematic errors, particularly for heavy precipitation estimation (Frank et al., 2018; Garibay et al., 2021; Hersbach et al., 2020; Parker, 2016; Probst & Mauser, 2022). Hence, it is necessary to rectify the bias associated with extreme precipitation values. To achieve this, the Annual Maximum Precipitation (AMP) series for 6-h, 12-h, 18-h and 24-h durations were extracted from both observed and ERA5 data. Then, the AMP series were subsequently arranged in descending order. The bias correction factor (f_{bc}) is established as the proportion of the th observed AMP ($\mathrm{AMP}_{Obs(i,j,l)}$) to the th ERA5 AMP ($\mathrm{AMP}_{ERA5(i,j,l)}$), as shown in the following Equation:

$$f_{bc} = \frac{\mathrm{AMP}_{Obs(i,j,l)}}{\mathrm{AMP}_{ERA5(i,j,l)}} \quad (1)$$

In this equation, i and j indicate the given station and duration, respectively. Afterward, the average factor is multiplied by the original ERA5 AMP data and the bias-corrected ERA5 AMP is obtained. By the above-mentioned method, the bias factors are estimated for the seven synoptic stations. However, we need the bias factor for each grid of the ERA5 data to have

a map of the IDF curves over the basin. As proposed by Noor et al., (2021), the obtained bias correction factor for the gauge stations can be related to the physiographic factors such as elevation. This relationship then can be applied for the ungauged areas based on their topography. Accordingly, in this study, a relationship between the bias factors and the elevations of the stations were developed. Then using the developed relationship and the elevations of the grid points, the bias factors for each grid point were estimated.

GEV Distribution

The Generalized Extreme Value (GEV) distribution is a widely employed statistical model in hydrology and extreme value analysis. The GEV distribution is a three-parameter family of continuous probability distributions which is defined as follows:

$$F(x) = \exp\left[-\left(1 + k\frac{(x-\mu)}{\sigma}\right)^{-\frac{1}{k}}\right] \quad (2)$$

where, $1 + k\frac{(x-\mu)}{\sigma} > 0$, k, μ, and σ are the shape, location, and scale parameters, respectively. The parameters have been estimated using the Maximum Likelihood Estimation (MLE) method at 95% confidence level (Hilbe & Robinson, 2013).

The suitability of the GEV distribution for modeling extreme events is rooted in its ability to describe the distribution of block maxima (Coles et al., 2001) including the AMP series. Previous studies have successfully applied the GEV distribution for development of the IDF curves (Cheng & AghaKouchak, 2015; Crévolin et al., 2023; Guhathakurta et al., 2011; Ragno et al., 2018; Shrestha et al., 2017). Recently, it has been used for extreme rainfall events modeling using the gridded rainfall data (Marra et al., 2017, 2019; Mianabadi, 2023; Noor et al., 2021; Ombadi et al., 2018; Venkatesh et al., 2022). Hence, the GEV distribution was also applied in this study, to fit the AMP series to develop the IDF curves.

The three parameters of k, μ, and σ are time-independent for a stationary GEV distribution, while the parameters are changing with time for the non-stationary distribution (Cheng & AghaKouchak, 2015; Coles et al., 2001). Srivastava et al. (2021) suggested that for the non-stationary distribution, the shape parameter is constant and the location and scale parameters is described as follows:

$$\mu(t) = \mu_0 + \mu_1 t \quad (3)$$

$$\sigma(t) = \sigma_0 + \sigma_1 t \quad (4)$$

In these equations, t is time and μ_0, μ_1, σ_0, and σ_1 are the regression coefficients.

It should be noted that the shape parameter of a non-stationary Generalized Extreme Value (GEV) distribution is typically assumed to be constant because it reflects the stable tail behavior of extreme events governed by fundamental physical laws. This assumption simplifies modeling and parameter estimation, while empirical

studies have consistently shown that the shape parameter remains stable over time, despite variability in the location and scale parameters (Barbero et al., 2017; De Leo et al., 2021; Luke et al., 2017).

To distinguish between the stationary and nonstationary GEV distribution, the trends in the AMP series should be analyzed. If the trend in the AMP series is significant/ insignificant at 95% confidence level, the GEV distribution is non-stationary/ stationary (Cheng & AghaKouchak, 2015; Ragno et al., 2018). More details on this issue is provided by Srivastava et al. (2021) and Cheng and AghaKouchak (2015). In this study, the Mann-Kendall (MK) trend test (Kendall, 1975; Mann, 1945) were used for trend analysis. The analysis was conducted by the "extRemes2.0" package in R (Gilleland & Katz, 2016).

Mann-Kendall Test for Trend Analysis

The Mann-Kendall (MK) test is commonly used to analyze the trend in hydrological and climatological time series. As a non-parametric test, it can be applied to all kind of probability distributions, meaning that the assumption of normality is not required for the data series. The Mann-Kendall test statistic is defined as follows:

$$z_{MK} = \begin{cases} \frac{S-1}{\sqrt{V(S)}} & if\ S > 0 \\ 0 & if\ S = 0 \\ \frac{S+1}{\sqrt{V(S)}} & if\ S < 0 \end{cases} \quad (5)$$

in which

$$S = \sum_{k=1}^{n-1} \sum_{j=k+1}^{n} \text{sign}(x_j - x_k) \quad (6)$$

$$V(S) = \frac{[n(n-1)(2n+5) - \sum_{i=1}^{m} t_i(t_i-1)(2t_i+5)]}{18} \quad (7)$$

with x_j and x_k the sequential data values, V(S) the variance of S, t_i the number of ties for the i-th value, n the number of data points, and m the number of tied groups. The positive/negative values of z_{MK} represent increasing/decreasing trends in the data series. The significant trends were considered at 90, 95, and 99% confidence interval, i.e., α=0.1, α=0.05, and α=0.01, respectively. The seasonal effect was considered for the series by seasonal decomposition method, but as the seasonal effect was not significant, we did not include it in the manuscript. Seasonal effect may result in significant trend in AMP series, but the trend is not significant in most areas of the basin and thus, the seasonal variability does not affect the trend in AMP.

Results and Discussion

Bias Correction

To extract the gridded data into the stations' locations, the nearest neighbor interpolation method was applied. Then the extracted data was compared to the measured data of the stations. Figures 2-5 illustrate the Q-Q plots comparing the quantiles of the AMP series before and after bias correction for 6-24 hourly precipitation, respectively. Beside Q-Q plot, the evaluation metrics have been also presented in Table 1. According to the

figures and table, in general, the original ERA5 performs better as the precipitation duration increase, however, the bias correction led to better estimation of AMP values, implying that it can remove a significant part of systematic errors (bias) in the ERA5 data (Ombadi et al., 2018). It leads to better estimation of IDF curves as illustrated in figure 6. As shown in this figure, the IDF curves developed by bias corrected ERA5 data is closer to the ones developed by measured data. It should be mentioned that the ERA5 IDF curves is closer to the measured one for the shorter return periods (i.e., 2, 5, and 10 years). Larger discrepancies for the return periods longer than the length of the data record were also reported by (Marra et al., 2017). Their results indicated the uncertainty for the return periods longer than twice the data record length (in this study, 50 and 100 years) might be up to 125%. The figure also shows that the IDF curves is more reliable for the 12, 18, and 24 h durations. Prein et al. (2015) suggested that ERA5 underestimates precipitation intensities at shorter duration because they are likely to be convective in nature and of limited spatial scale. This is important due to the fact that ERA5 does not directly assimilate any rain-gauge data, but it estimates precipitation through modelling process (Courty et al., 2019; Lavers et al., 2022). Marra et al. (2017) indicated that the gridded precipitation products are reliable for IDF development for 12-24 h durations and 2-10 years return periods, which are more applicable for flood management and infrastructures design. Among the study stations, Ilam, Kermanshah, and Khoramabad show the worst performance of the original ERA5. These stations with high elevations (1337, 1318.5, and 1147.8 m, respectively) receive the highest amount of annual precipitation during 1996-2020 (560, 414, and 478 mm, respectively) in the study area. Hence, it indicates that the ERA5 does not perform well for the high-altitude stations with the high amount of precipitation. Such results also found by Kavyani Malayeri et al., (2021).

Additionally, the discrepancy between measured and simulated extreme precipitation might be due to the smoothing effect (Hamm et al., 2020; Herrera et al., 2012; Merino et al., 2021; Reder et al., 2022; Wati et al., 2022). A grid point of the gridded products has the information of an area, according to the spatial resolution (for ERA5 31km×31km). Averaging the information from that area into a point may affect the amount of estimated precipitation.

Elevation-Bias Factor Relationship

Table 2 shows the elevation and the bias factors of the seven stations. According to this table, the correlation between elevation and bias factors are provided as illustrated in figure 7. The figure shows

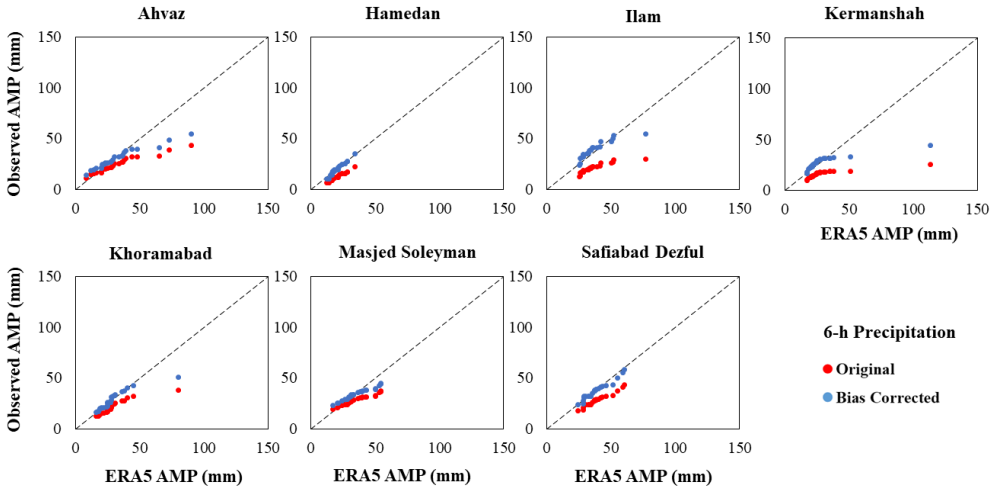

Fig 2. Q-Q plot of observed 6-h AMP vs ERA5 6-h AMP for each station before and after bias correction.

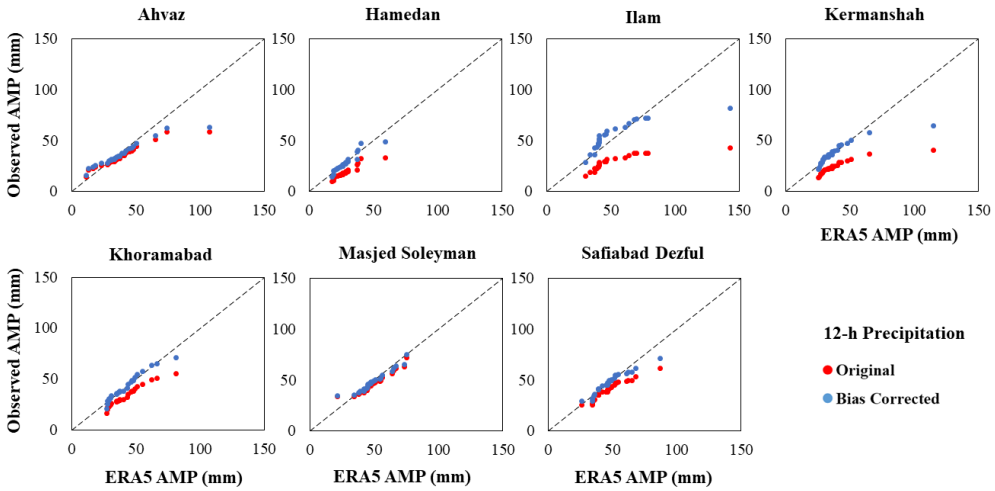

Fig 3. Q-Q plot of observed 12-h AMP vs ERA5 12-h AMP for each station before and after bias correction.

a reasonable correlation as R^2 varies between 0.52 to 0.74 for 6-24 hourly AMP. As indicated by Ombadi et al., (2018), these correlations show that 52 to 74 percent of the variability in the bias is explained linearly by elevation. It can be concluded that the ERA5 precipitation tends to have higher bias in the high-altitude areas. Such results also found by Jiao et al., (2021) and Kavyani Malayeri et al., (2021). The statistical significance of Pearson correlation coefficient has been investigated and presented in Table 2. As shown in Table 2, the Pearson correlation is significant at 95% confidence level (P_value<0.05). Hence, the elevation-bias factor relationship can be applied for all grid points of the basin.

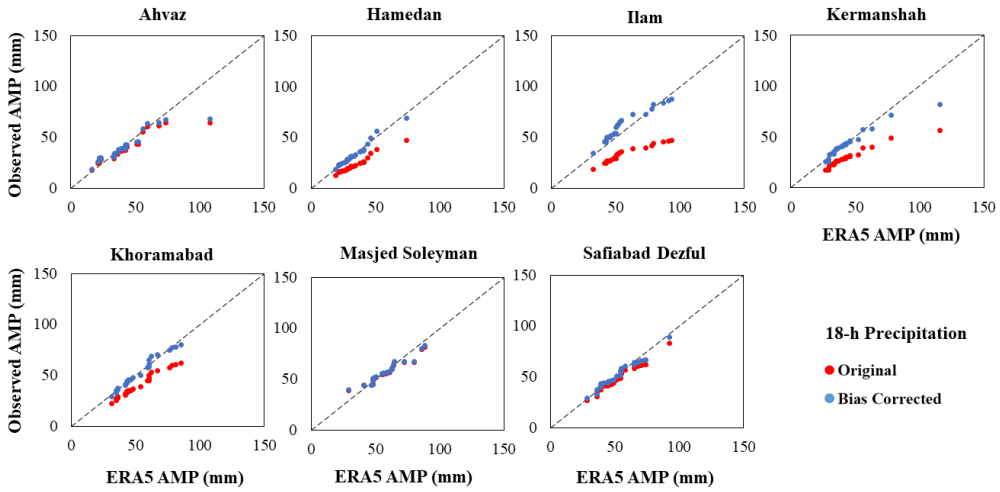

Fig 4. Q-Q plot of observed 18-h AMP vs ERA5 18-h AMP for each station before and after bias correction.

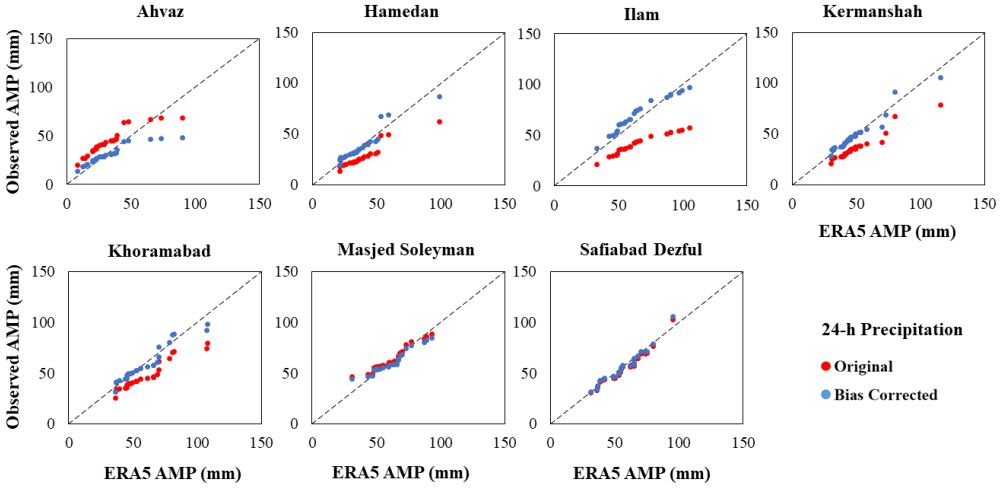

Fig 5. Q-Q plot of observed 24-h AMP vs ERA5 24-h AMP for each station before and after bias correction.

Trend Analysis

As indicated earlier, to choose between the stationary or non-stationary GEV distribution function, it is needed to analyze the trends in the AMP series for each grid point. Figure 8 shows the spatial distribution of the across the KRB. As seen in the figure, some limited grid points in the northeast show significant trends in the 6-h and 12-h AMP series at 95% confidence level. For these grid points the non-stationary GEV distribution function should be fitted to the AMP series. For the other grid points the stationary GEV was applied.

IDF development for the KRB

Spatial distribution of rainfall intensity (mm/h) for different return periods has been illustrated in figures 9-12 for

Table 1- Evaluation metrics for 6-h, 12-h, 18-h, and 24-h AMP series before and after bias correction.

Station	Evaluation Metric	6-h		12-h		18-h		24-h	
		Original	Bias corrected	Original	Bias corrected	Original	Bias corrected	Original	Bias corrected
Ahvaz	MAE	9.0	5.9	6.6	5.1	5.2	4.4	13.1	6.4
	RMSE	14.3	10.3	11.2	9.9	9.7	8.8	13.7	11.0
Hamedan	MAE	7.1	0.9	8.8	1.9	10.5	1.5	10.9	3.4
	RMSE	7.3	1.1	9.7	3.0	11.4	2.1	12.7	5.0
Ilam	MAE	20.3	9.7	30.2	14.6	34.8	15.2	35.0	15.6
	RMSE	34.8	25.8	48.9	33.9	54.7	36.3	54.2	35.3
Kermanshah	MAE	12.8	6.4	14.7	4.2	14.4	3.3	13.1	2.7
	RMSE	20.6	14.5	19.5	10.4	17.6	7.0	14.7	4.4
Khoramabad	MAE	7.4	2.5	8.9	2.0	11.8	1.8	11.8	4.5
	RMSE	10.3	5.9	9.8	2.8	12.5	2.5	13.8	5.6
Masjed Soleyman	MAE	6.9	4.1	3.4	2.1	3.1	3.0	3.9	4.0
	RMSE	8.8	5.2	4.5	3.6	4.3	4.2	5.2	4.9
Safiabad Dezful	MAE	9.8	1.8	6.9	3.1	4.0	2.5	3.3	3.0
	RMSE	10.6	2.3	8.6	4.2	5.1	3.0	4.0	3.7

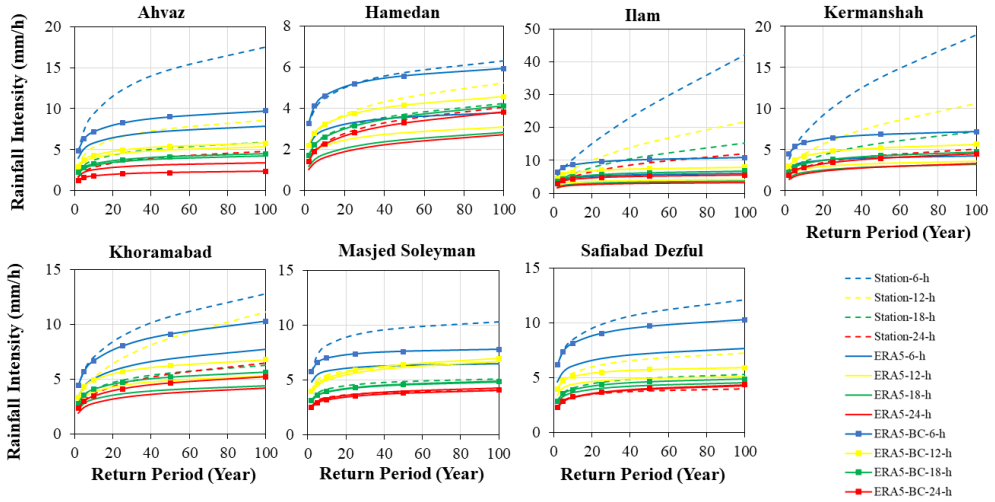

Fig 6. IDF curves developed by measured, ERA5, and ERA5 bias corrected AMP series. The term "BC" indicates the Bias Corrected ERA5.

Table 2- Relationship between elevation and bias factor for each station and precipitation duration.

Station	Elevation (m)	Bias Factor			
		6-h	12-h	18-h	24-h
Ahvaz	22.5	1.25	1.07	1.05	0.69
Hamedan	1740.8	1.56	1.47	1.45	1.40
Ilam	1337	1.82	1.89	1.85	1.70
Kermanshah	1318.5	1.70	1.28	1.45	1.35
Khorramabad	1147.8	1.33	1.58	1.29	1.24
Masjed Soleyman	320.5	1.20	1.04	1.01	0.96
Safiabad Dezful	82.9	1.34	1.16	1.07	1.03

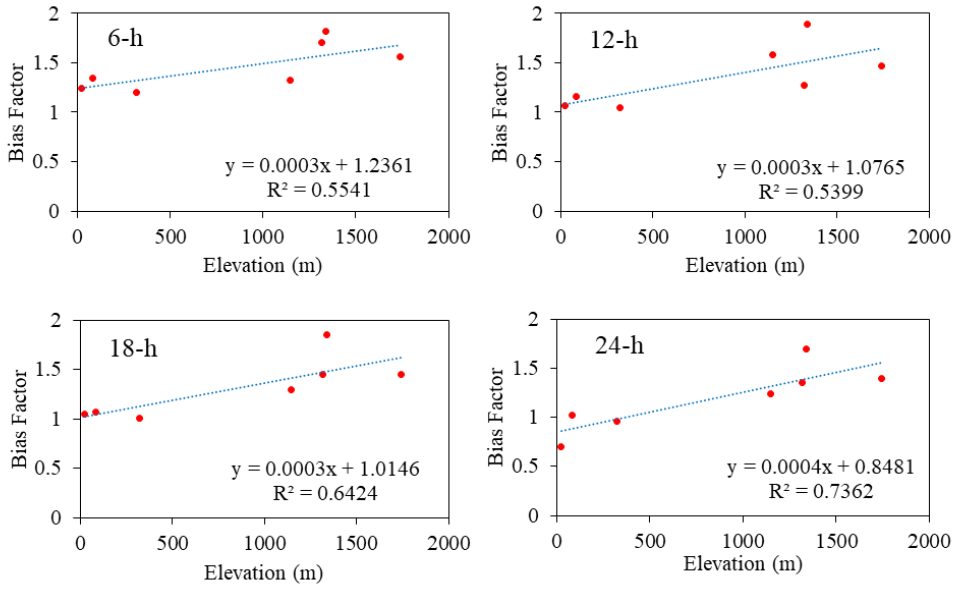

Fig 7. Correlation between elevation and bias factor for different precipitation durations.

Table 2- Statistical significance test of the Pearson correlation between elevation and Bias factor.

Station	Elevation (m)	Bias Factor			
		6-h	12-h	18-h	24-h
Ahvaz	22.5	1.25	1.07	1.05	0.69
Hamedan	1740.8	1.56	1.47	1.45	1.40
Ilam	1337	1.82	1.89	1.85	1.70
Kermanshah	1318.5	1.70	1.28	1.45	1.35
Khorramabad	1147.8	1.33	1.58	1.29	1.24
Masjed Soleyman	320.5	1.20	1.04	1.01	0.96
Safiabad Dezful	82.9	1.34	1.16	1.07	1.03

*: Significant at 95% confidence level.

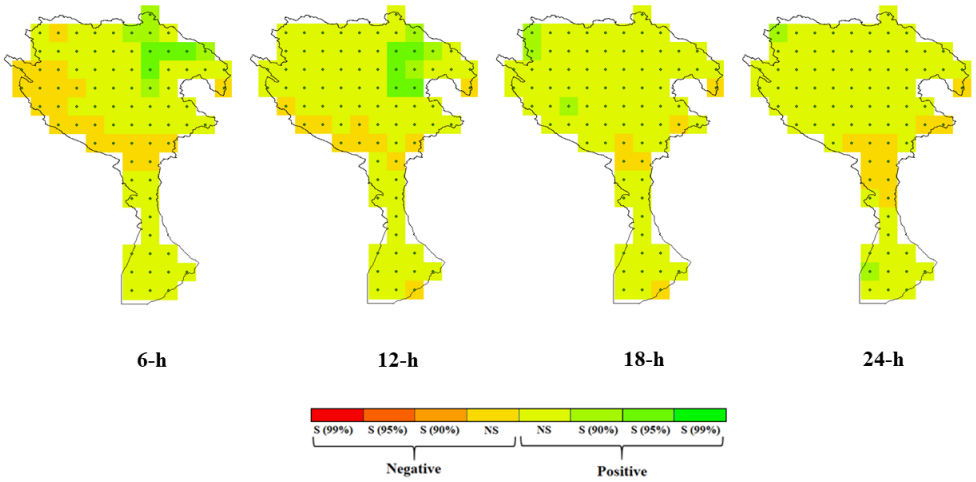

Fig 8. Spatial distribution of the Z_{MK} and significance of the trends in KRB.

6-24 hourly precipitation, respectively. According to these figures, the rainfall intensity has the similar patterns for each duration and return period. The rainfall is more intense in the high-altitude regions of the KRB. Based on these figures, the intensity, duration and return period for each grid point can be acquired. Marra et al. (2017) pointed out that the distance from the rain gauge location reduces the repre-sentativeness of the gauge-acquired IDF curves. Thus, for constructing the infrastructures, the policy makers can use the information of the closer grid points to the location of the infrastructures rather than that of the distant rain gauges.

Spatial analysis of Figures 9 to 12 indicates that the highest rainfall intensities for various durations and return periods are concentrated in the eastern, southeastern, and central parts of the basin, corresponding to the Kashkan sub-basin. This sub-basin, identified by Azadi et al. (2020) as having the highest flood potential in the KRB, underscores the critical importance of accurate IDF estimates in these areas due to their heightened sensitivity to flooding. The comprehensive IDF curves of the KRB is presented in figure 13. As seen in the figure, the curves of each return period are relatively equally spaced. It means the difference between rainfall intensities for different return periods is constant during all rainfall durations. Wambura (2024) believed that this constant difference might be due to using the same probability distribution function for all series, while the series might be fitted with different functions. Since the curves are provided by the bias corrected precipitation data of 82 points, it may be more reliable than the curves acquired from only seven stations within or around the KRB. Moreover, the IDF curves can be developed for each grid point, as it can be more helpful for infrastructures design in each location across the basin.

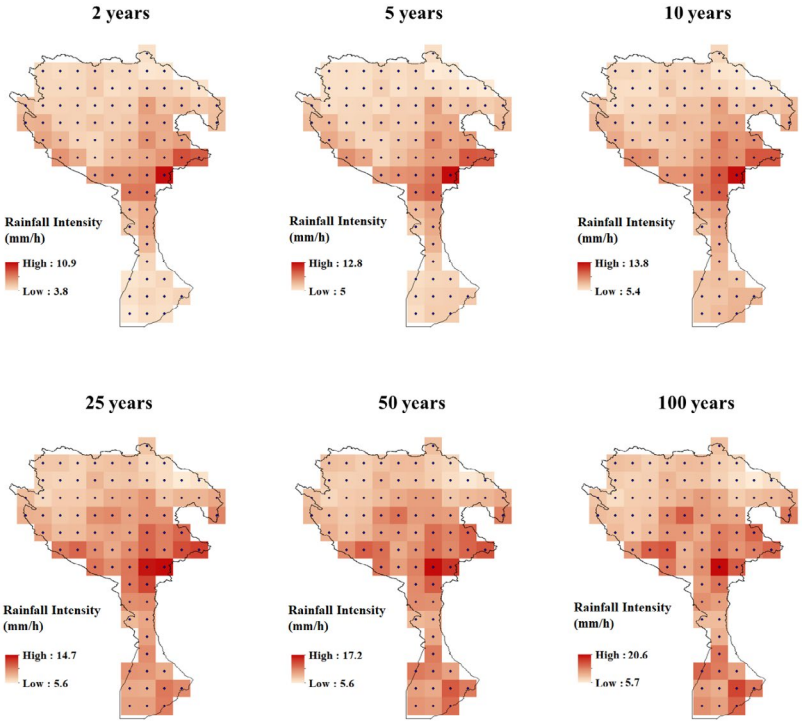

Fig 9. Spatial distribution of 6-h rainfall intensity for different return periods over the KRB.

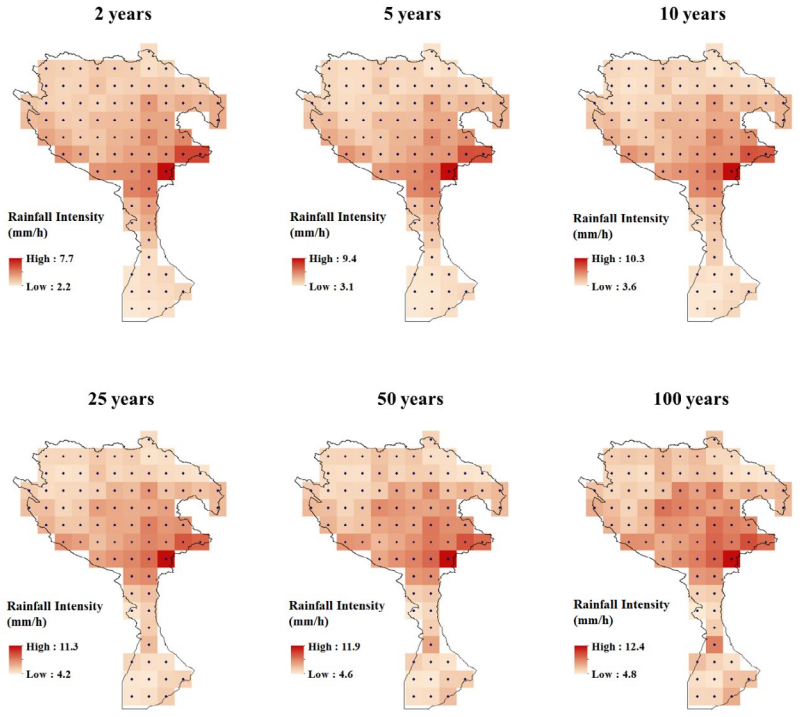

Fig 10. Spatial distribution of 12-h rainfall intensity for different return periods over the KRB.

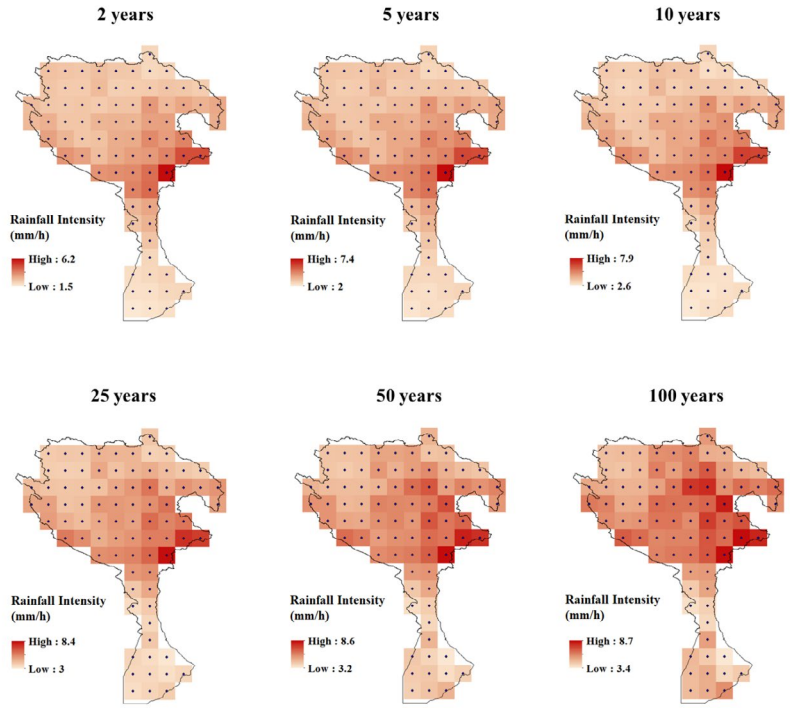

Fig 11. Spatial distribution of 18-h rainfall intensity for different return periods over the KRB.

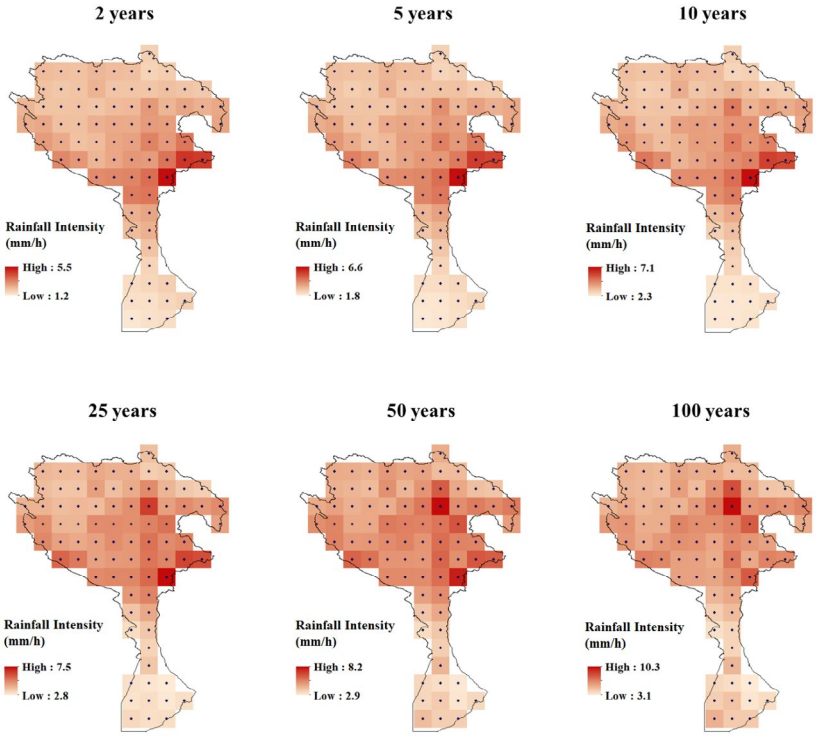

Fig 12. Spatial distribution of 24-h rainfall intensity for different return periods over the KRB.

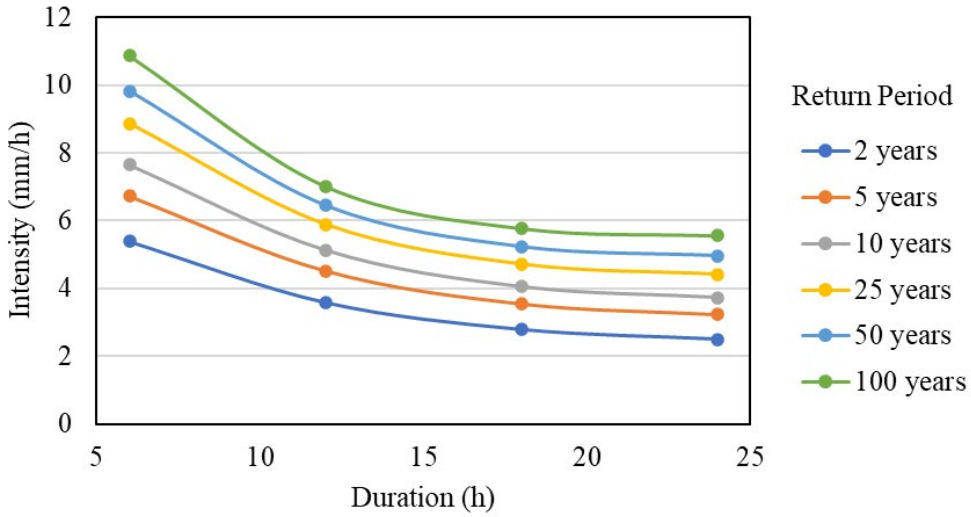

Fig 13. IDF curve of the KRB developed by the ERA5 database.

Conclusion

This study developed Intensity-Duration-Frequency (IDF) curves for the Karkheh River Basin (KRB) using ERA5 reanalysis data, supported by bias correction with observed precipitation data. The analysis revealed that bias correction significantly improves ERA5 estimates, particularly for high-altitude regions prone to systematic errors. The relationship between bias factors and elevation was effectively utilized to extend bias correction across the basin. Furthermore, the use of the Generalized Extreme Value (GEV) distribution, incorporating both stationary and non-stationary trends, provided a robust framework for modeling extreme precipitation.

While this study demonstrates the potential of ERA5 data to enhance hydrological analyses, it acknowledges limitations such as the short observational record (25 years), which reduces the accuracy of rainfall intensity estimates for longer return periods e.g., 50 and 100 years. Future research should address this limitation and uncertainties by extending data records, refining bias correction methods, exploring alternative datasets, and evaluating uncertainties related to interpolation techniques, parameter estimation, and distribution fitting.

By providing a framework for utilizing ERA5 reanalysis data for spatially comprehensive IDF curve development, this study contributes to more reliable flood mitigation strategies, climate-resilient infrastructure planning, and improved adaptation to the impact of climate change particularly in data-scarce regions. Policymakers and engineers are encouraged to utilize these updated IDF curves to inform decision-making processes that enhance resilience against extreme weather events.

References

Ashraf Vaghefi, S., Mousavi, S. J., Abbaspour, K. C., Srinivasan, R., & Yang, H. (2014). Analyses of the impact of climate change on water resources components, drought and wheat yield in semiarid regions: Karkheh River Basin in Iran. Hydrological Processes, 28(4), 2018–2032. https://doi.org/10.1002/hyp.9747

Azadi, F., Sadough, S. H., Ghahroudi, M., & Shahabi, H. (2020). Zoning of flood risk in kashkan river basin using two models WOE and EBF. Journal of Geography and Environmental Hazards, 9(1), 45–60. [In Persian]. https://doi.org/ 10.22067/GEO.V9I1.83090.

Barbero, R., Fowler, H. J., Lenderink, G., & Blenkinsop, S. (2017). Is the intensification of precipitation extremes with global warming better detected at hourly than daily resolutions? Geophysical Research Letters, 44(2), 974–983. https://doi.org/10.1002/2016GL071917

Cheng, L., & AghaKouchak, A. (2015). Nonstationary precipitation intensity-duration-frequency curves for infrastructure design in a changing climate. Scientific Reports, 4(1), 7093. https://doi.org/10.1038/srep07093

Coles, S., Bawa, J., Trenner, L., & Dorazio, P. (2001). An introduction to statistical modeling of extreme values. Springer London. https://doi.org/10.1007/978-1-4471-3675-0

Courty, L. G., Wilby, R. L., Hillier, J. K., & Slater, L. J. (2019). Intensity-duration-frequency curves at the global scale. Environmental Research Letters, 14(8), 084045. https://doi.org/10.1088/1748-9326/ab370a

Crévolin, V., Hassanzadeh, E., & Bourdeau-Goulet, S.-C. (2023). Updating the intensity-duration-frequency curves in major Canadian cities under changing climate using CMIP5 and CMIP6 model projections. Sustainable Cities and Society, 92(September 2022), 104473. https://doi.org/10.1016/j.scs.2023.104473

Davtalab, R., Mirchi, A., Khatami, S., Gyawali, R., Massah, A., Farajzadeh, M., & Madani, K. (2017). Improving continuous hydrologic modeling of data-poor river basins using hydrologic engineering center's hydrologic modeling system: case study of karkheh river Basin. Journal of Hydrologic Engineering, 22(8). https://doi.org/10.1061/(ASCE)HE.1943-5584.0001525

De Leo, F., Besio, G., Briganti, R., & Vanem, E. (2021). Non-stationary extreme value analysis of sea states based on linear trends. Analysis of annual maxima series of significant wave height and peak period in the Mediterranean Sea. Coastal Engineering, 167, 103896. https://doi.org/10.1016/j.coastaleng.2021.103896

Frank, C. W., Wahl, S., Keller, J. D., Pospichal, B., Hense, A., & Crewell, S. (2018). Bias correction of a novel European reanalysis data set for solar energy applications. Solar Energy, 164, 12–24. https://doi.org/10.1016/j.solener.2018.02.012

Garibay, V. M., Gitau, M. W., Kiggundu, N., Moriasi, D., & Mishili, F. (2021). Evaluation of reanalysis precipitation data and potential bias correction methods for use in data-scarce areas. Water Resources Management, 35(5), 1587–1602. https://doi.org/10.1007/s11269-021-02804-8

Gilleland, E., & Katz, R. W. (2016). ExtRemes 2.0: an extreme value analysis package in R. Journal of Statistical Software, 72(8), 1–39. https://doi.org/10.18637/jss.v072.i08

Guhathakurta, P., Sreejith, O. P., & Menon, P. A. (2011). Impact of climate change on extreme rainfall events and flood risk in India. Journal

of Earth System Science, 120(3), 359–373.
Hersbach, H., Bell, B., Berrisford, P., Biavati, G., Horányi, A., Muñoz Sabater, J., Nicolas, J., Peubey, C., Radu, R., Rozum, I., Schepers, D., Simmons, A., Soci, C., Dee, D., & Thépaut, J.-N. (2023). ERA5 hourly data on single levels from 1940 to present. Copernicus Climate Change Service (C3S) Climate Data Store (CDS). https://doi.org/10.24381/cds.adbb2d47
Hersbach, H., Bell, B., Berrisford, P., Hirahara, S., Horányi, A., Muñoz-Sabater, J., Nicolas, J., Peubey, C., Radu, R., Schepers, D., Simmons, A., Soci, C., Abdalla, S., Abellan, X., Balsamo, G., Bechtold, P., Biavati, G., Bidlot, J., Bonavita, M., … Thépaut, J. (2020). The ERA5 global reanalysis. Quarterly Journal of the Royal Meteorological Society, 146(730), 1999–2049. https://doi.org/10.1002/qj.3803
Hilbe, J. M., & Robinson, A. P. (2013). Methods of statistical model estimation. CRC Press.
IPCC. (2021). Technical summary. contribution of working group I to the sixth assessment report of the Intergovernmental panel on climate change. In climate change 2021: The Physical Science Basis.
Jalbert, J., Genest, C., & Perreault, L. (2022). Interpolation of precipitation extremes on a large domain toward IDF curve construction at unmonitored locations. Journal of Agricultural, Biological and Environmental Statistics, 27(3), 461–486. https://doi.org/10.1007/s13253-022-00491-5
Jiao, D., Xu, N., Yang, F., & Xu, K. (2021). Evaluation of spatial-temporal variation performance of ERA5 precipitation data in China. Scientific Reports, 11(1), 17956. https://doi.org/10.1038/s41598-021-97432-y
Kavyani Malayeri, A., Saghafian, B., & Raziei, T. (2021). Performance evaluation of ERA5 precipitation estimates across Iran. Arabian Journal of Geosciences, 14(23), 2676. https://doi.org/10.1007/s12517-021-09079-8
Kendall, M. G. (1975). Rank Correlation Methods. Charles Griffin.
Koutsoyiannis, D., Kozonis, D., & Manetas, A. (1998). A mathematical framework for studying rainfall intensity-duration-frequency relationships. Journal of Hydrology, 206(1–2), 118–135. https://doi.org/10.1016/S0022-1694(98)00097-3
Lavers, D. A., Simmons, A., Vamborg, F., & Rodwell, M. J. (2022). An evaluation of ERA5 precipitation for climate monitoring. Quarterly Journal of the Royal Meteorological Society, 148(748), 3152–3165. https://doi.org/10.1002/qj.4351
Luke, A., Vrugt, J. A., AghaKouchak, A., Matthew, R., & Sanders, B. F. (2017). Predicting nonstationary flood frequencies: Evidence supports an updated stationarity thesis in the <scp>U</scp> nited <scp>S</scp> tates. Water Resources Research, 53(7), 5469–5494. https://doi.org/10.1002/2016WR019676
Mann, H. B. (1945). Nonparametric Tests Against Trend. Econometrica, 13(3), 245–259.
Marra, F., Morin, E., Peleg, N., Mei, Y., & Anagnostou, E. N. (2017). Intensity–duration–frequency curves from remote sensing rainfall estimates: comparing satellite and weather radar over the eastern Mediterranean. Hydrology and Earth System Sciences, 21(5), 2389–2404. https://doi.org/10.5194/hess-21-2389-2017
Marra, F., Nikolopoulos, E. I., Anagnostou, E. N., Bárdossy, A., & Morin, E. (2019). Precipitation frequency analysis from remotely sensed datasets: A focused review. Journal of Hydrology, 574, 699–705. https://doi.

org/10.1016/j.jhydrol.2019.04.081

Mianabadi, A. (2023). Evaluation of long-term satellite-based precipitation products for developing intensity-frequency (IF) curves of daily precipitation. Atmospheric Research, 286(February), 106667. https://doi.org/10.1016/j.atmosres.2023.106667

Noor, M., Ismail, T., Shahid, S., Asaduzzaman, M., & Dewan, A. (2021). Evaluating intensity-duration-frequency (IDF) curves of satellite-based precipitation datasets in Peninsular Malaysia. Atmospheric Research, 248, 105203. https://doi.org/10.1016/j.atmosres.2020.105203

Ombadi, M., Nguyen, P., Sorooshian, S., & Hsu, K. (2018). Developing intensity-duration-frequency (IDF) curves from satellite-based precipitation: Methodology and Evaluation. Water Resources Research, 54(10), 7752–7766. https://doi.org/10.1029/2018WR022929

Parker, W. S. (2016). Reanalyses and Observations: What's the difference? Bulletin of the American Meteorological Society, 97(9), 1565–1572. https://doi.org/10.1175/BAMS-D-14-00226.1

Prein, A. F., Langhans, W., Fosser, G., Ferrone, A., Ban, N., Goergen, K., Keller, M., Tölle, M., Gutjahr, O., Feser, F., Brisson, E., Kollet, S., Schmidli, J., van Lipzig, N. P. M., & Leung, R. (2015). A review on regional convection-permitting climate modeling: Demonstrations, prospects, and challenges. Reviews of Geophysics, 53(2), 323–361. https://doi.org/10.1002/2014RG000475

Probst, E., & Mauser, W. (2022). Evaluation of ERA5 and WFDE5 forcing data for hydrological modelling and the impact of bias correction with regional climatologies: A case study in the Danube River Basin. Journal of Hydrology: Regional Studies, 40, 101023. https://doi.org/10.1016/j.ejrh.2022.101023

Ragno, E., AghaKouchak, A., Love, C. A., Cheng, L., Vahedifard, F., & Lima, C. H. R. (2018). Quantifying changes in future intensity-duration-frequency curves using multimodel ensemble simulations. Water Resources Research, 54(3), 1751–1764. https://doi.org/10.1002/2017WR021975

Shrestha, A., Babel, M., Weesakul, S., & Vojinovic, Z. (2017). Developing intensity–duration–frequency (IDF) curves under climate change uncertainty: The Case of Bangkok, Thailand. Water, 9(2), 1–22. https://doi.org/10.3390/w9020145

Srivastava, A. K., Grotjahn, R., Ullrich, P. A., & Sadegh, M. (2021). Pooling data improves multimodel IDF estimates over median-based IDF estimates: Analysis over the Susquehanna and Florida. Journal of Hydrometeorology, 22(4), 971–995. https://doi.org/10.1175/JHM-D-20-0180.1

Tarek, M., Brissette, F. P., & Arsenault, R. (2020). Evaluation of the ERA5 reanalysis as a potential reference dataset for hydrological modelling over North America. Hydrology and Earth System Sciences, 24(5), 2527–2544. https://doi.org/10.5194/hess-24-2527-2020

Venkatesh, K., Maheswaran, R., & Devacharan, J. (2022). Framework for developing IDF curves using satellite precipitation: a case study using GPM-IMERG V6 data. Earth Science Informatics, 15(1), 671–687. https://doi.org/10.1007/s12145-021-00708-0

Wambura, F. J. (2024). Using reanalysis precipitation data for developing intensity-duration-frequency curves in a poorly gauged city. Journal of Hydrology: Regional Studies, 56, 102005. https://doi.org/10.1016/j.

ejrh.2024.102005

Zambrano-Bigiarini, M., Soto, C., & Tolorza, V. (2024). Spatially-distributed intensity-duration-frequency (IDF) curves for chile using sub-daily gridded datasets. EGU general assembly 2024, Vienna, Austria, 14–19 Apr 2024. https://doi.org/10.5194/egusphere-egu24-21043